IMPACT OF MULTI-AXIAL STRESSES ON ASR EXPANSION

Pierre Morenon[1,2*], Stéphane Multon[2], Alain Sellier[2], Etienne Grimal[1], François Hamon[3], Eric Bourdarot[1]

[1]Electricité de France, Centre d'Ingénierie Hydraulique, EDF-CIH Technolac, 73373 Le Bourget du Lac Cedex, FRANCE

[2]Université de Toulouse, UPS, INSA, LMDC (Laboratoire Matériaux et Durabilité des constructions), 135, avenue de Rangueil, F-31 077 Toulouse Cedex 04, FRANCE

[3]Electricité de France, Direction Etude et Recherche, EDF-DER, 1 avenue du Général de Gaulle, 92141 Clamart Cedex, FRANCE

Abstract

Among large civil engineering structures, some concrete dams are submitted to structural effects of Alkali-Silica Reaction (ASR). This is mainly due to the concrete composition and climatic conditions such as water supply. Thus, Electricité de France (EDF), the most important dam owner in France, has supported the ASR modelling development, in collaboration with the LMDC Toulouse for the last decades in order to ensure dams safety and optimize maintenance.

In this work, the aim is to show how restraints can modify ASR expansions. The behaviour of concrete submitted to ASR under multi-axial loading is modelled in the poro-mechanical framework. It contains a creep model which allows a realistic interaction between ASR and structural behaviour to be considered. Furthermore, the mechanical part considers anisotropic damage of affected concrete and includes cracks reclosure. The model is also able to dissociate expansion micro-cracks and structural macro-cracks.

An analysis of literature experiments is performed by using a model to simulate swelling cylinders under restraint. In these tests, specimens are loaded in uniaxial compression and the radial displacement is restrained by steel rings surrounding concrete cylinders. A global calibration is realised in order to validate the model with all restraints and loads.

After the modelling fitting and validation, parametric study is performed in order to assess uni-axial behaviour of affected concrete in various loading conditions. Maximal stresses and damages are thus analysed. Finally, useful practical considerations for engineering are deduced. They can be used in order to help experts for the management of ASR damaged structures.

Keywords: Alkali-Silica Reaction, concrete modelling, stresses effects, anisotropy

1 INTRODUCTION

Alkali-Silica Reaction expansion occurs in structures which sustain significant loads like bridge pier or are restrained by external loading conditions such as dams in valleys. Moreover, restrain of expansion by reinforcement and prestressing in structures cause also stresses during expansion. In order to manage the damaged structures, owners need confident tools to predict future damages. ASR free stress swelling has been largely studied and several models reproduce the phenomenon realistically. Despite of the number of experiment, ASR swelling under restrain has not yet been fully understood and modelled.

The aim of this work is to show how restraints can modify ASR expansions. After model explanation, parameters are fitted and validated on a literature multi-axial restrained experiment [1,2]. Based on this calibration, a parametric study is conducted in order to assess uniaxial behaviour of affected concrete in various loading conditions. Maximal stresses and damages are specially focused to obtain useful practical considerations for engineering.

2 MODELLING

2.1 State of art

For a long time, authors tried to understand and to predict ASR under loading and its effects on structures.

* Correspondence to: morenon@insa-toulouse.fr

A lot of them experiment directly ASR expansion in order to find out the maximum mechanical gel pressure. Uniaxial stress application is the most common test. Expansions on mortar [3,4] or on concrete [1,2,3] show a stress between 0.4 to 10 MPa under several environmental conditions and aggregate types. Some experiments on mortar and on concrete were lead on multi-axial stresses or restraints [1,2]. Expressed maximal mechanical stresses vary from 1 to 14 MPa.

Expansion is due to ASR gel pressure: understanding the effect of stresses of this pressure is one of the most important problems to solve. Once the chemical kinetics known, the question is to know if there is a maximum chemical gel pressure value which can stop the ASR-development. To calculate this chemical gel pressure, several equations are used in the literature. Equation 1 comes from Correns [5] and Scherer [6] works.

$$\mathrm{P} = -\frac{\mathrm{R\,T\ln(Q/K)}}{\nu} \tag{1}$$

$$2\,SiO_2(aq) + 3H_2O + (Na^{+} or\ K^{+}) + HO^{-} \rightleftharpoons (N\ or\ K)HSi_2O_5.3H_2O \tag{2}$$

R is the gas constant (8.3145 J.K^{-1}.mol^{-1}), T is the absolute temperature and ν the molar volume of the crystal (around 20 cm^3.mol^{-1} for calcic gels [7]). K is the equilibrium constant (10$^{-4.6}$ for Na-S-H and 10$^{-5.005}$ for K-S-H [8]) of the gel creation (Equation 2). Q can be defined as the ionic activity product of the gel creation (Equation 3). The theoretical chemical pressure exerted by the crystal on the solid skeleton can be calculated.

$$Q = [SiO_2]^2.[K^{+}].[HO^{-}] \tag{3}$$

If $[\mathrm{SiO_2}]$ and $[\mathrm{K^+}]$ are around 1 mol/L and $[HO^{-}]$ is around 0.3 mol/L (it corresponds to pH=13.5), then the pressure required to stop the crystal growth is upper than 300 MPa.

The difference between theoretical chemical calculus and mechanical experiments results shows that the maximum chemical pressure is never reached in all the concrete. External in situ stresses should not affect gel production because the needed stress to stop swelling is really upper than concrete strength. Extremely locally, the external stress may involve a very important stress value (>100 MPa). If the crystallisation is impossible there, ions migrate in the initial porosity or in cracks and will cause the crystallisation elsewhere in the concrete. Crystallisation is a little bit postponed.

2.2 ASR modelling

Chemical advancement

ASR advancement A^{asr} varies from 0 (before the start of the reaction) to 1 (when the reaction ends). Its evolution principally depends on the temperature and the humidity of the material (Equation 4). τ_{ref}^{asr} is a characteristic time which gives a mean representation of the different mechanisms of ASR-gels production (diffusive phenomenon and silica reactivity). It can be obtained by calibration on measured expansion. $A^{asr\,\infty}$ is the maximal advancement value reachable according to environmental conditions. It can be equal to saturation degree because only water sites can interact in ASR-gels development [9].

$$\frac{\delta A^{asr}}{\delta t} = \frac{1}{\tau_{ref}^{asr}} C^{T,asr} C^{W,asr} (A^{asr\,\infty} - A^{asr}) \tag{4}$$

Temperature effect ($C^{T,asr}$) is managed by an Arrhenius' law (Equation 5), where E^{asr} is the chemical activation energy (≈ 40,000 J/Mol [3]) and T_{ref} the reference temperature for which τ_{ref}^{asr} has been set.

$$C^{T,asr} = \exp\left(-\frac{E^{asr}}{R}\left(\frac{1}{T} - \frac{1}{T_{ref}}\right)\right) \tag{5}$$

When the material is not saturated, reaction kinetics is slowed down. The parameter $C^{W,asr}$ manages this phenomenon (Equation 6). S_r represents the saturation degree and $S_r^{th,asr}$ the saturation degree threshold below which the reaction stops. Then, the fraction of gel produced by the reaction is ϕ_g. It is the product between the advancement and the maximum gel potential ϕ_g^{∞} (Equation 7).

$$C^{W,asr} = \begin{cases} \dfrac{S_r - S_r^{th,asr}}{1 - S_r^{th,asr}} & if \quad S_r > S_r^{th,asr} \\ 0 & if \quad S_r \leq S_r^{th,asr} \end{cases} \tag{6}$$

$$\phi_g = \phi_g^{\infty}.A^{asr} \tag{7}$$

ASR mechanical effects

Gel exerts a pressure P_g (Equation 8) on aggregate and concrete. In this modelling, P_g is the average pressure transferred to the aggregate surface. It mainly depends on the accessible porosity, the initial one or the one created by strains (elastic or plastic).

$$P_g = M_g\left(\phi_g - \left(\phi_g^v\left(\frac{P_g}{P_g^{lim}}\right) + b_g tr(\varepsilon - \varepsilon^{p,g}) + tr(\varepsilon^{p,g})\right)\right) \tag{8}$$

M_g is the gel modulus. ϕ_g^v is a fraction of non-efficient gel to create expansion under the characteristic pressure P_g^{lim}. This last one is the necessary pressure to micro-crack the solid skeleton (equation 9). It usually depends on the effective tensile strength $\tilde{R}_I^t$ (Equation 9) and on k_g which represents the stress concentration factor (which depends on aggregate shape). This parameter fits the local strength to intra-porous gel pressure.

$$P_g^{lim} = \frac{\tilde{R}_I^t}{k_g} \tag{9}$$

P_g expression (Equation 8) is managed in two main parts. The first one is the non-efficient gel creation, transcribed by $\phi_g^v\left(\frac{P_g}{P_g^{lim}}\right)$. P_g^{lim} is the necessary pressure to begin the micro-cracking of a concrete element free of stress. When $P_g > P_g^{lim}$ (triaxial restraint for example), the gel spreads on the connected porosity under pressure. The second part of the expression is the volume $b_g tr(\varepsilon - \varepsilon^{p,g}) + tr(\varepsilon^{p,g})$ which represents the porosity created by strains which absorbs a part of the gel without creating pressure. The entire volume created by strains (except the ASR plastic volume) is affected by the Biot coefficient b_g which comes from poromechanics considerations [10,11]. Indeed, $b_g tr(\varepsilon)$ represents the variation of the porosity volume filled by ASR-gel under concrete strain. Grimal's model [12] gives calibration of b_g lying between 0.1 and 0.4. For plastic strains induced by the ASR $(\varepsilon^{p,g})$, b_g=1 because cracks created by the gel are supposed to be always accessible for the gel and then totally filled by it (Figure 1).

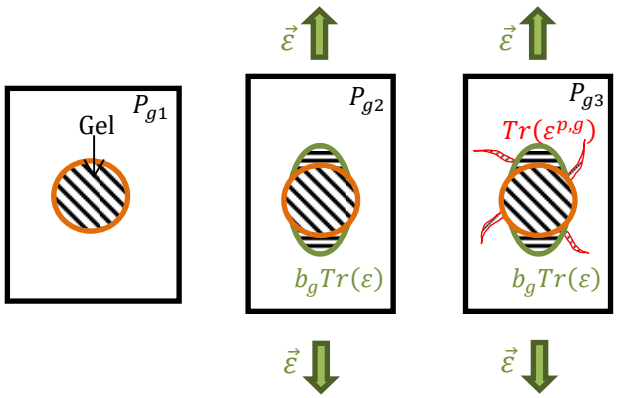

For A^{aar} = constant, $P_{g1} > P_{g2} > P_{g3}$

FIGURE 1: Strains effects on gel pressure. $b_g Tr(\varepsilon)$ is the variation of the porosity due to concrete strain. $Tr(\varepsilon^{p,g})$ is the variation of the porosity due to plastic ASR-strains.

The concrete behaviour is modelled in the poro-mechanical framework. The model contains a damage model [13], and a creep model which considers a realistic interaction between ASR and structural behaviour. Creep model, which is a Burger chain, is explained in [12]. Concrete shrinkage during the same period can also be taken into account. This paper focuses on ASR modelling including ASR pressure and kinetics, and their links to plasticity.

The non-linear mechanical part describes the material behaviour by using anisotropic plastic criteria and damages. In order to calculate plastic strains, there are two criteria groups: one to manage shear cracking (Drucker Prager criteria) which is isotropic, and one to operate traction behaviour (Rankine criteria) which is orthotropic. This last one separates structure macro-cracks, reclosing macro-cracks and intra-porous pressure micro-cracks (ASR).

P_g (Equation 8) is used to determinate micro-cracking due to ASR by a special criterion f_I^g which takes into account the stress state. $\tilde{\sigma}_I$ is the principal tensile stress in direction I.

$$\begin{cases} \mathrm{f_I^g} = \mathrm{k_g P_g} & if \quad \tilde{\sigma}_\mathrm{I} \geq \tilde{\mathrm{R}}_\mathrm{I}^\mathrm{t} \\ \mathrm{f_I^g} = \mathrm{k_g P_g} + \tilde{\sigma}_\mathrm{I} - \tilde{\mathrm{R}}_\mathrm{I}^\mathrm{t} & if \quad \tilde{\sigma}_\mathrm{I} < \tilde{\mathrm{R}}_\mathrm{I}^\mathrm{t} \end{cases} \text{ with I} \in \text{[I,II,III]} \tag{9}$$

The hardening law which links ASR pressure to ASR strain can be drawn with a bilinear curve (Figure 2). $\mathrm{E_c}$ represents the concrete Young modulus and $\mathrm{H_{asr}}$ the plastic hardening ratio ($\mathrm{h_{asr}}.\mathrm{Ec}$ is the hardening modulus) to ASR plastic criteria. During free swelling, when the gel pressure reaches P_g^{lim}, ASR induces the creation of micro-cracks fulfilled by the gel. The corresponding strains are modelled using plastic strains. A h_{asr} close to 0 means that when P_g^{lim} is reached, plastic ASR strains rise very quickly and, as $\mathrm{P_g}$ is proportional to h_{asr}, the gel pressure stays close to the limit pressure. If h_{asr} is larger (>0.1), the ASR plastic strains are possible only if the gel pressure increases, and the micro-cracking induced by the gel is stable.

When a compression stress is applied to concrete ($\sigma < 0$), cracking first appears in perpendicular loaded direction (Figure 3). Then P_g increases, depending on h_{asr} value. If $\tilde{\mathrm{R}}_\mathrm{I}^\mathrm{g} - \sigma$ is reached, cracking can be initialized in the loaded direction.

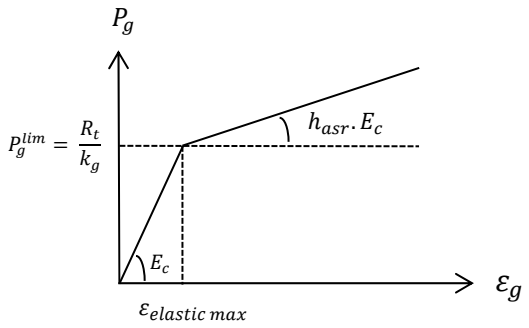

FIGURE 2: Plastic ASR hardening law.

Anisotropic cracking had been observed in several experiments. In free swelling tests, cracks are spread in all directions. Once specimens are loaded, cracking is oriented perpendicularly to the loaded direction (Figure 4). The anisotropy of cracking leads to the anisotropy of resulting expansion, usually observed during expansion under loading.

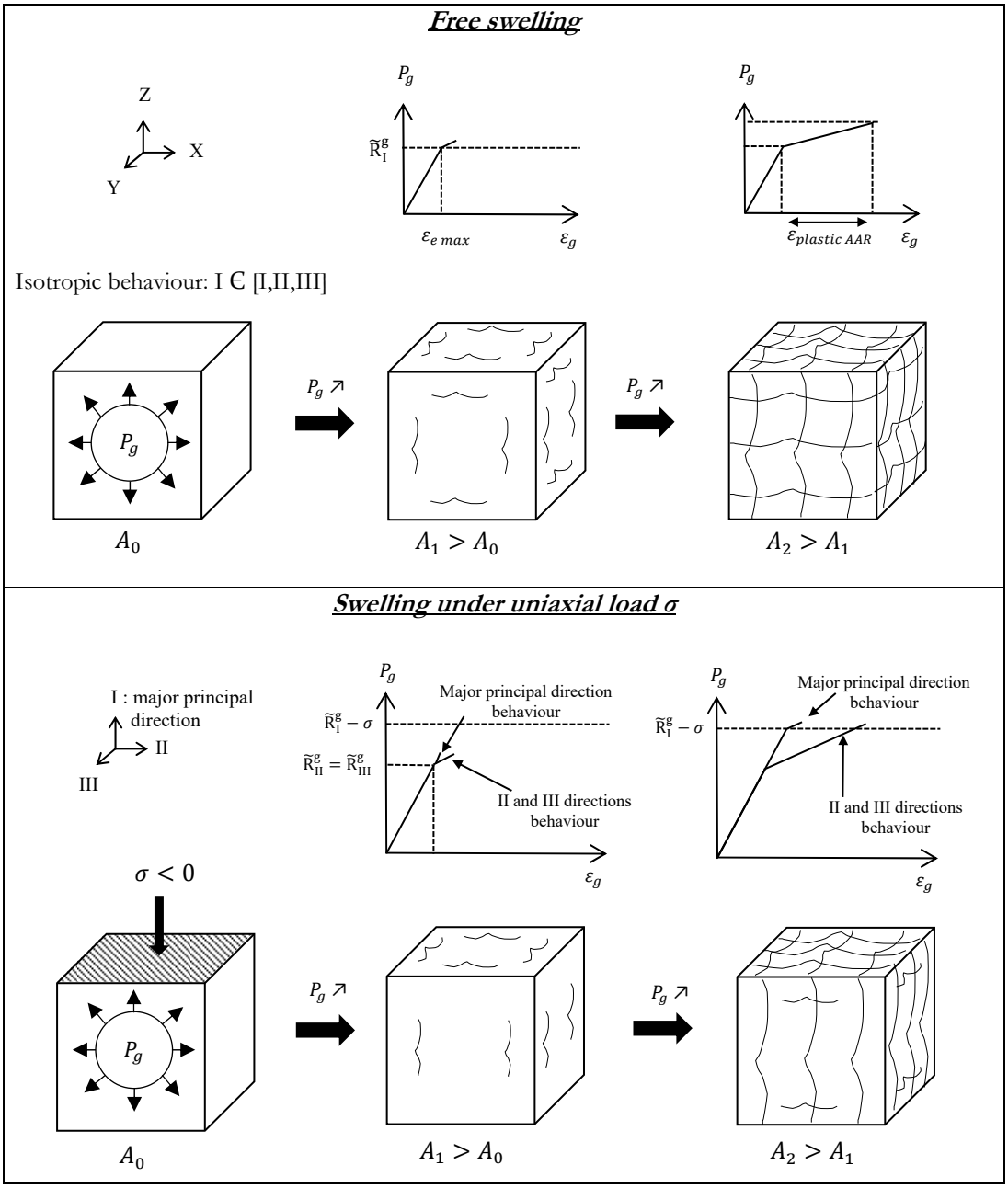

FIGURE 3: Loading effects on cracking direction on specimen affected by ASR.

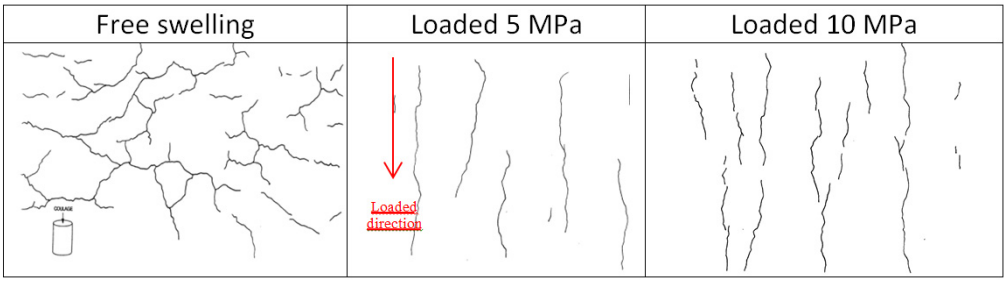

FIGURE 4: ASR specimens cracking appearance due to several loadings [3].

3 Modelling validation and analysis

3.1 Modelling validation on Multon's test

Fitting on Multon's tests [1] is performed in order to validate the model. In this experiment, specimens were loaded in uniaxial compression and the radial displacement was restrained by steel rings surrounding concrete cylinders. After fitting creep and shrinkage, the first step is the calibration. A global calibration is realised in order to validate the model with all restraints and loads.

Creep and shrinkage are fitted on non-reactive specimen (Figure 5). Shrinkage cylinders were sealed with three aluminium layers. From the mass loss, the environmental conditions and the fitting strains are reproduced faithfully. Then, creep tests at 10 and 20 MPa enable to simulate the material behaviour under long time loading. For all Multon's tests, a 28 days curing period is applied at 20°C. Then, the temperature increases to 38°C. Results are presented after the curing period.

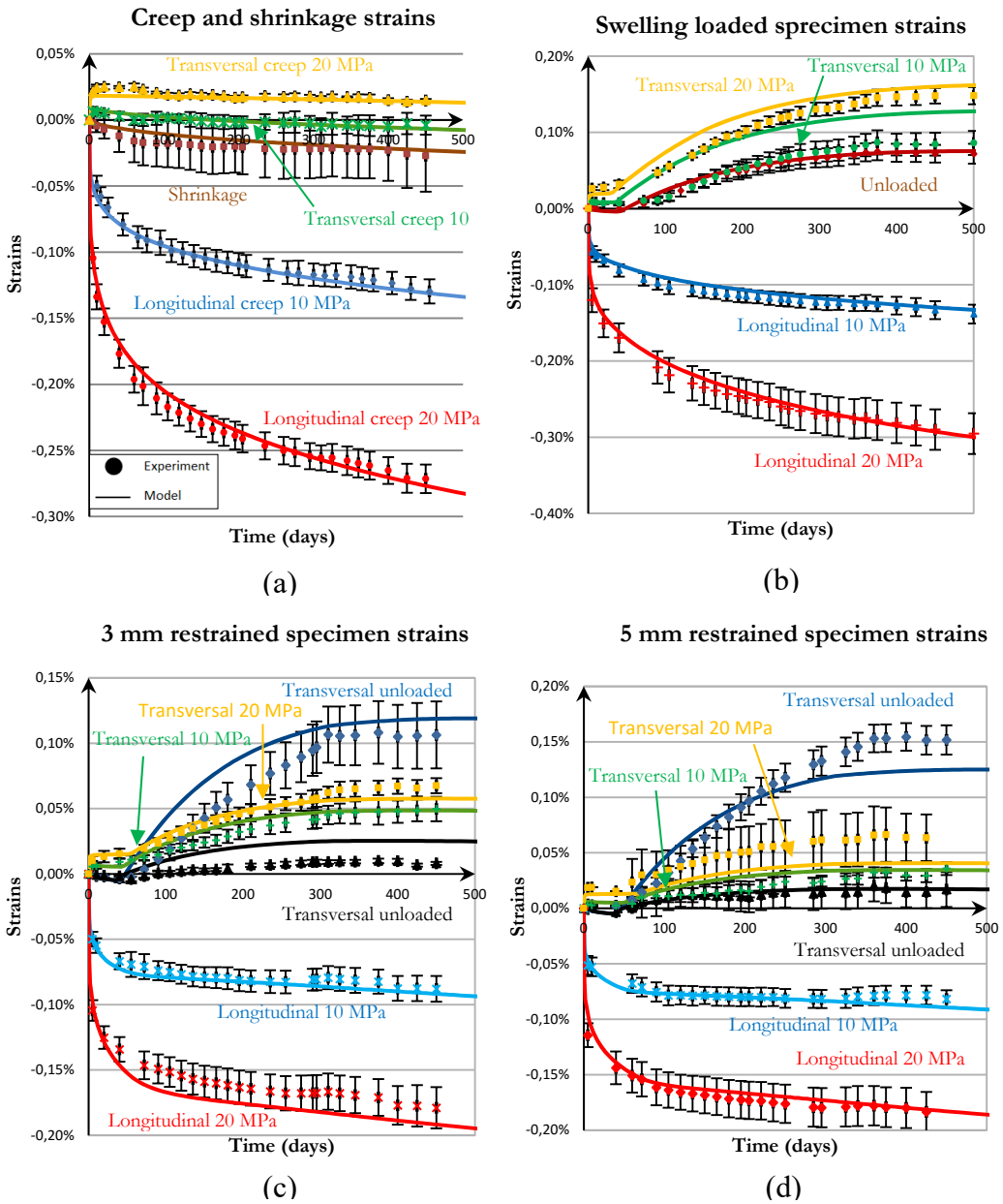

FIGURE 5: Multon's tests [1]: (a) creep and shrinkage without ASR, (b) ASR free swelling tests, (c) 3 mm restrained tests, (d) 5 mm restrained tests (R_t=3.7 MPa; $\boldsymbol{\phi}_{\mathbf{g}}^{\infty}$=0.0078 m³/m³; $\boldsymbol{\phi}_{\boldsymbol{g}}^{\boldsymbol{v}}$=0.00148 m³/m³ bg=0.25; M_g=27700 MPa; H_{asr}=0.1).

Then, a free-swelling test gives strains to calibrate ASR criteria such as maximal ASR product ratio ϕ_g^∞, volume of unexpansive ASR phase ϕ_g^v and Biot ASR coefficient b_g (Figure 5). Furthermore, swelling tests under restrain (radial displacement is restrained by 3 mm or 5 mm steel rings) are used to find ASR Biot modulus M_g and the stress concentration factor k_g.

3.2 Discussion on validation tests

Figure 5 shows that the model is able to reproduce ASR expansions under multi-axial loads and restraints, and to approach experimental results.

Specimens are loaded in uniaxial compression and the radial displacement is restrained by steel rings surrounding concrete cylinders. Due to ASR expansion and Poisson effect on loaded tests, radial stresses are developed on these rings. These stresses are extracted from the calculus (Figure 6). Model results give radial stresses from 2.2 to 6.0 MPa. Radial stress curves contain four parts: the external stress application (between 0 and 1 day), the latency period before expansion begins to be significant (between 1 and 80 days), the expansion period (between 80 and 350 days) and the part where reaction is over and shrinkage becomes the main phenomenon of deformation.

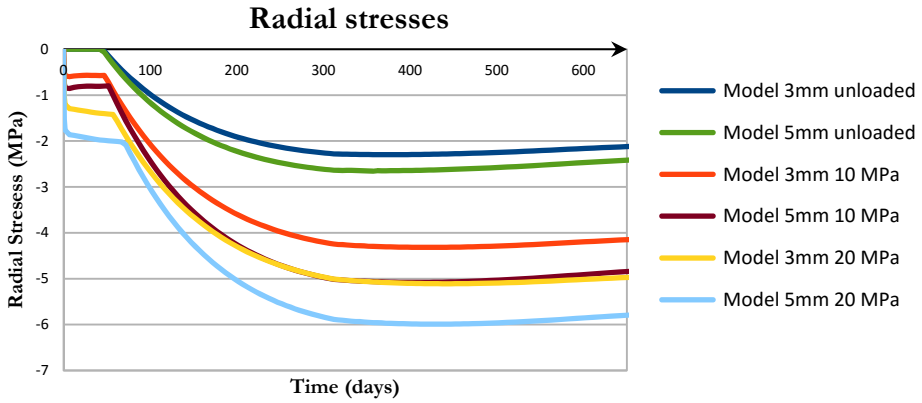

FIGURE 6: Radial stresses obtained from the model.

During the latency period, radial stress is nearly zero for unloaded specimens because shrinkage is more important than gel pressure, so concrete and steel rings are not in contact. Specimens with 3 mm steel rings got a smaller radial stress because of rings rigidity.

Then, the expansion beginning depends on applied stress. Indeed, strains are taken into account in P_g equation. The increase of the stress in 5 mm steel rings is more significant because the rigidity slows the radial strain (for the same stress applied). The more restrained the cylinder is, the quicker the radial stress increases (Figure 7). At 650 days, the gel pressure which represents the average pressure transferred to the aggregate surface varies from 8.2 MPa to 12.2 MPa according to stress state.

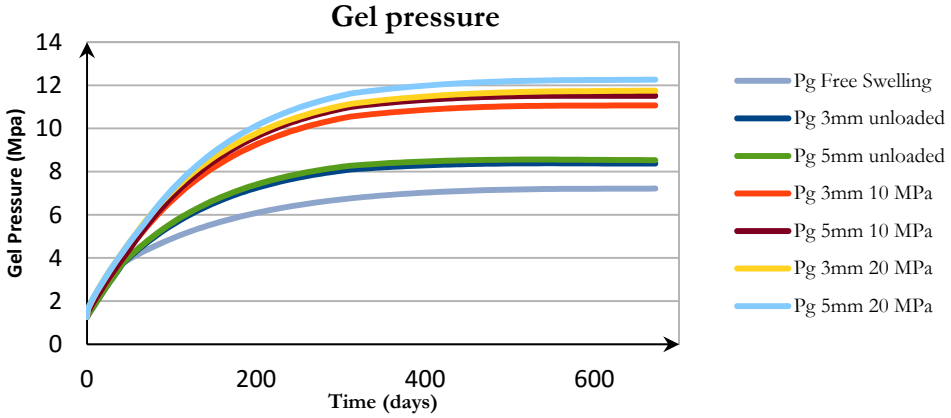

FIGURE 7: Gel pressure from the model in restrained tests.

4 Theoretical case studies

4.1 Unidirectional tests

In this part, a theoretical test is performed in order to analyse the effects of restraint and stress on ASR-expansion. A cube is submitted to several uniaxial loading conditions (Figure 8): free swelling, swelling under a perfect restraint in one direction and swelling under several stresses. Impacts will be analysed in terms of expansion, stress and damage. In order to analyse the concrete behaviour under the only pressure of ASR, tests are calculated without shrinkage. Stresses are applied after 28 days.

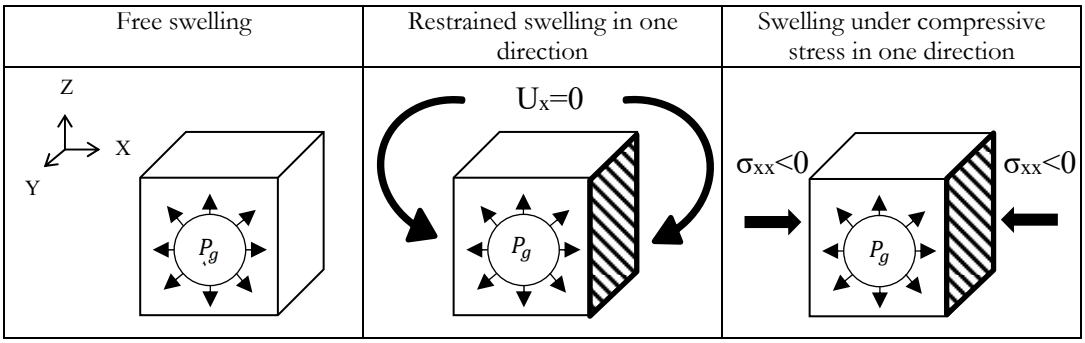

FIGURE 8: Conditions of theoretical tests.

4.2 Theoretical analyses of the impact of stress on ASR-expansion

After running free swelling test and a one-direction perfectly restrained expansion test, stresses in direction XX are extracted (Figure 9). In Figure 9, the stress in restrained conditions can be described in two phases: a slow increase of the stress before first cracking (0 to 80 days), then the stress increases fast after first ASR damage. For this condition of perfect restraint, the maximal stress reaches about 3 MPa of compression. If the free maximal strain is 0.1%, an isotropic thermo-elastic calculus gives a stress of 37.7 MPa ($E_c.\varepsilon$=37700 * 0.001). Taking into account usual creep (E_c= E_{c0}/3), result still gives 12.6 MPa. These results are not consistent with experimental results, as seen in the state of the art.

The decrease of the stress after 500 days is due to stress relaxation obtained in the calculation by the coupling with creep. To complete this theoretical analysis, stresses lying between 0 MPa and the maximal stress obtained under the perfect restraint are applied (between 0 MPa and 3.5 MPa).

Figure 11 shows the strains obtained for the different loadings. The larger the applied stress is, the smaller the final strain is. Upper 1 MPa of compressive stress, the latency period depends on stress state because creep strains are larger than the strains induced by the gel pressure. This varies from 60 to 295 days. For the 3 MPa test (nearly the maximum pressure obtained on the restrained test), the final strain is nearly 0. Modelling is thus consistent when expansions under restraint and under loading are compared.

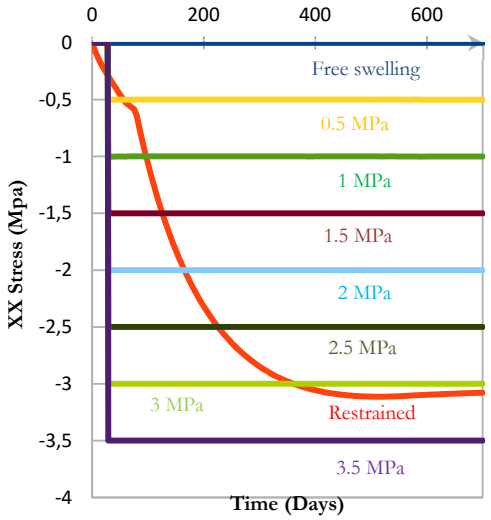

FIGURE 9: Stresses in direction XX (MPa).

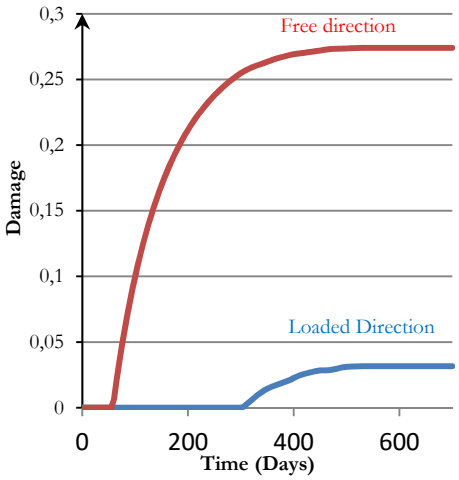

FIGURE 10: Damages in the 3.5 MPa Loading Test.

Figure 10 shows the damages in loaded and free directions for the 3.5 MPa loading test. The first damaged direction is the unloaded one, and then, the direction loaded is slightly damaged (here $h_{asr} = 0.1$). There is a delay between the cracking in each direction, as explained in Figure 3. The free direction is less damaged than loaded direction. The difference depends directly on the stress applied. For a smaller stress, the damage perpendicular to the loaded direction will be greater, while for a stress upper than about 4 MPa, it can be expected to obtain no damage perpendicular to the loaded direction. As damage affects directly the Young modulus, the material becomes anisotropic; the Young modulus will be smaller in the free direction while the mechanical performances are less affected in loaded ones.

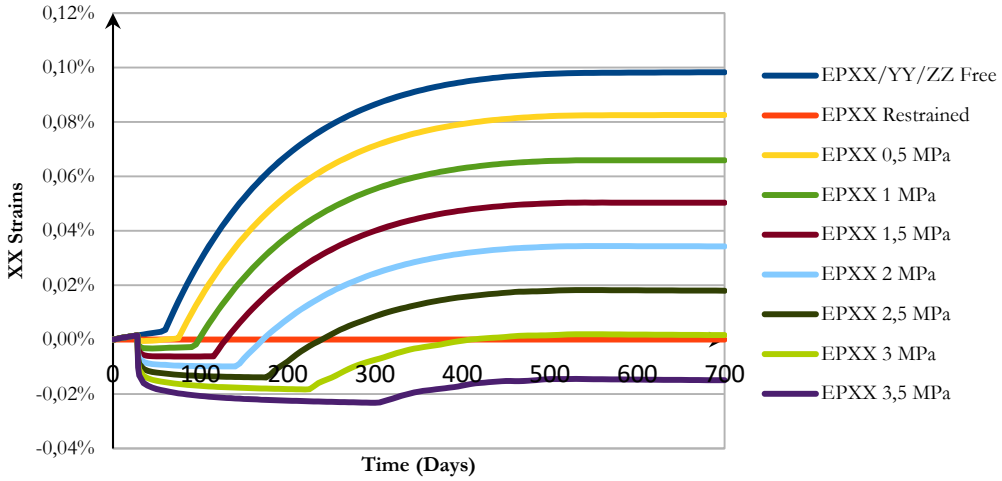

FIGURE 11: Strains in direction XX.

4.3 Guidance for structural analysis

Anisotropic cracking of ASR affected concrete should be in the centre of structural expert attention. Damage direction depends on loaded directions which vary on each kind of structures. Although ASR free swelling cracking can be supposed mainly isotropic or at least random, cracking in loaded structures is largely influenced by main stress directions. In gravity dams, upstream-downstream direction is more loaded than perpendicular directions. In arch dams, vertical direction is less loaded than ortho-radial directions.

Therefore, Young modulus obtained on core sampling drilled from damaged structures can depend on coring direction, especially on strong anisotropic stressed structure. The larger damage can be expected in free directions which are not the most important directions for the mechanical analysis of the structures. Experts of ASR damaged structures management have to be aware of this characteristic during the core test analysis. Young modulus extracts may not be appropriate to model the material in all directions.

The residual swelling test consists in quantifying the remaining expansion of existing structure at the present time. Cores are extracted from the structure and tested on free swelling on laboratory under specific conditions to accelerate expansion. Results will be impacted by the direction of cracks in the cores. Indeed, gel created can be partly accommodated by the cracks and the test will not lead to the same results according to the directions of measurement compared to cracks directions. Thus, the drilling direction can modify the structural analysis.

5 CONCLUSIONS

The aim of this paper was to show how restraints and stresses can modify ASR expansions. First, a theoretical pressure calculus was lead in order to know what could be the maximum chemical pressure. Analytic calculus based on chemical considerations only gives a gel pressure of 300 MPa while stresses in concrete cannot be upper than its strength. However, some extensions (cracking, creep, etc) can limit the gel pressure increase.

The model used takes into account some physics phenomena such as creep and damage. Attention is focused on the gel pressure calculus and on the hardening law chooses to manage the cracking due to ASR. Gel pressure calculus includes elastic strains and ASR plastic strains respecting poromechanics principles.

The model is calibrated and validated on experimental results [1,2]. Specimen are tested under several mechanical conditions: creep and shrinkage without ASR, free swelling with or without loads, restrained swellings (cylinders inside steel rings 3 and 5 mm thick) with or without load. Numerical results show a realistic behaviour compared to experimental results. The average gel pressure at the scale of concrete is about 8 MPa for free expansion and does not exceed 12.2 MPa for loaded and restraint specimens.

Based on that, a theoretical test is lead. The main goal is to compare ASR swelling under restraint and swelling under stress. A cube is subjected to one direction restrained swelling. Restrained direction stress is extracted to apply it to a new cube without restraint. Conclusions show that final strains are the same but kinetics is different due to the loading chronology. With those material parameters, a compressive stress of 3 MPa is needed to obtain the same final strains. Results analysis reveals the anisotropic cracking behaviour of the ASR affected concrete under uniaxial stress. This phenomenon leads to give some guidance to experts for the management of ASR damaged structures. Indeed, coring direction can imply results differences on the analysis of anisotropic loaded structures.

To go further, it will be interesting to perform other theoretical tests in biaxial and triaxial conditions.

6 REFERENCES

[1] Multon, S., & Toutlemonde, F. (2006): Effect of applied stresses on alkali–silica reaction-induced expansions. Cement and Concrete Research, 36(5), 912-920.

[2] Multon, S. (2003): Evaluation expérimentale et théorique des effets mécaniques de l'alcali-réaction sur des structures modèles. Thesis, Université Marne La Vallée, France.

[3] Larive, C. (1997) : « Apports combinés de l'expérimentation et de la modélisation à la compréhension de l'alcali-réaction et de ses effets mécaniques », Thesis, Thèse de doctorat de l'Ecole Nationale des Ponts et Chaussées.

[4] Durand, B., & Chen, H. (1991). Preventive measures against alkali-aggregate reactions. Course Manual, Petrography and Alkali-Aggregate Reactivity, 399-489.

[5] Correns, C.W. (1949): Growth and dissolution of crystals under linear pressure, Disc. Faraday Soc. 5, 267–271.

[6] Scherer, G.W. (2004): Stress from crystallization of salt, Cement Concr. Res. 34 1613–1624.

[7] Perruchot, A., Massard, P., & Lombardi, J. (2003): Composition et volume molaire apparent des gels Ca Si, une approche expérimentale. Comptes Rendus Geoscience, 335(13), 951-958.

[8] Kim, T. & Olek, J. (2014): Chemical Sequence and Kinetics of Alkali–Silica Reaction Part II. A Thermodynamic Model. Journal of the American Ceramic Society, 97(7), pp. 2204-2212.

[9] Poyet, S. (2003): « Etude de la dégradation des ouvrages en béton atteints par la réaction alcali silice: Approche expérimentale et modélisation numérique multi-échelles des dégradations dans un environnement hydro-chemo-mécanique variable », thèse de doctorat de l'université de Marne la Vallée.

[10] Biot, M.A. (1972): Theory of finite deformation of porous solids. Indiana Univ. Math. J. 21, 579–620.

[11] Coussy, O. (1995): « Mechanics of Porous Continua », J. Wiley & Sons, Chichester, UK.

[12] Grimal, É., Sellier, A., Le Pape, Y., & Bourdarot, É. (2008): Creep, shrinkage, and anisotropic damage in alkali-aggregate reaction swelling mechanism-Part I: A constitutive model. ACI Materials Journal, 105(3).

[13] Sellier, A., Casaux-Ginestet, G., Buffo-Lacarrière, L., & Bourbon, X. (2013): Orthotropic damage coupled with localized crack reclosure processing. Part I: Constitutive laws. Engineering Fracture Mechanics, 97, 148-167.